Graphene

DOI: 10.1002/anie.200902365

A Strategy for Producing Pure Single-Layer Graphene Sheets Based on a Confined Self-Assembly Approach**

*Weixia Zhang, Jiecheng Cui, Cheng-an Tao, Yiguang Wu, Zhanping Li, Li Ma, Yuquan Wen, and Guangtao Li**

Owing to graphene's unusual physicochemical properties and tremendous potential for applications in nanoelectronics, sensors, nanocomposites, batteries, supercapacitors, and hydrogen storage, the development of efficient approaches to producing single-layer graphene sheets has been intensively explored in recent years.[1–4] Micromechanical cleavage from bulk graphite was initially used to produce graphene flakes, but the yield of this method is extremely low and the process is hard to control.[5] Recently, more efforts have been reported to isolate graphene sheets based on exfoliation or chemical oxidation of graphite or heat treatment of silicon carbide.[6–11] However, the uncontrollable character of these methods and in some cases the associated harsh conditions strongly restrict the quality of the resulting graphene materials and consequently limit their applications. For example, only moderate yields of single-layer graphene are obtained, while owing to the presence of foreign groups or stabilizers the obtained materials often exhibit a thickness more than 1 nm, which is much larger than that of clean graphene sheets. Thus, searching for a more efficient method to fabricate clean and pure graphene in bulk quantities is still highly desirable and urgent.

Herein, we describe a new strategy for producing high-quality single-layer graphene sheets using a confined self-assembly approach within lamellar mesostructured silica. Different from the above-mentioned top-down approaches, the bottom-up method demonstrated herein is characterized by the following features: first, the entire preparation process proceeds under mild conditions, and no hazardous agents are involved; second, this method allows fabrication of pure single-layer graphene sheets (100% yield, i.e. all of the prepared graphene sheets are single layers) with a thickness of 0.6 nm; third, graphene sheets with micrometer size are easily available, and their suspensions in aqueous solution show impressive long-term stability; finally, the procedure is controllable and can be used to produce graphene on a gram scale. It should be noted that, owing to the presence of defects in the nanosheet, the terminology "graphene-like" is more precise for the description of the prepared product. For conciseness, however, the term "graphene" is used to describe the product material.

Figure 1 displays the overall production strategy. A special structure-directing surfactant containing a pyrrole moiety is used to construct lamellar mesostructured silica. Since polypyrrole is an ideal carbon precursor to form graphite, this surfactant can serve simultaneously both as the structure-directing agent and as the carbon source. During the formation of the lamellar silica framework, the pyrrole moieties could be densely packed in a controlled fashion within confined 2D spaces between silica layers, providing the prerequisite for quantitative production of isolated graphene sheets after carbonization. After the in situ polymerization of the organized pyrrole moieties using $FeCl_3$ as oxidant, the resulting polypyrrole nanosheets were individually transformed into single-layer graphene sheets in N_2 atmosphere, for which the residual iron salts from the polymerization process were directly employed as catalyst for the conversion. Clearly, this three-step procedure provides a controllable, rational route for obtaining large, clean, and pure graphene sheets.

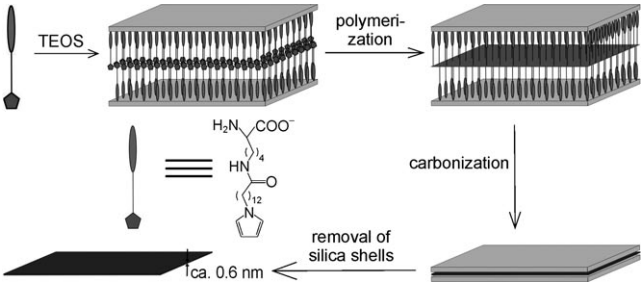

Figure 1. Schematic illustration of the fabrication of pure single-layer graphene with a thickness of about 0.6 nm. TEOS = tetraethoxysilane.

In our case, a lysine-based surfactant bearing a terminal pyrrole moiety ($PyC_{12}Lys$) was used as the structure-directing agent for the preparation of carbon-source-filled lamellar mesoporous silica (see the Experimental Section for a typical synthesis). Figure 2 shows the powder X-ray diffraction (XRD) pattern of the resultant silica materials prepared using $PyC_{12}Lys$ as the structure-directing agent from a reaction mixture with a molar composition of 1 TEOS/

[*] W. Zhang, J. Cui, C. Tao, Y. Wu, Dr. Z. Li, Prof. Dr. G. Li
Department of Chemistry, Key Lab of Organic Optoelectronics & Molecular Engineering, Tsinghua University
Beijing, 100084 (China)
Fax: (+86) 10-6279-2905
E-mail: lgt@mail.tsinghua.edu.cn
L. Ma, Prof. Dr. Y. Wen
State Key Laboratory of Explosion Science and Technology
Beijing Institute of Technology, Beijing, 100081 (China)

[**] We gratefully acknowledge the financial support from the National Science Foundation of China (20533050, 20772071, 50673048), transregional Project (TRR6) and 973 Program (2006CB806200).
Supporting information for this article is available on the WWW under http://dx.doi.org/10.1002/anie.200902365.

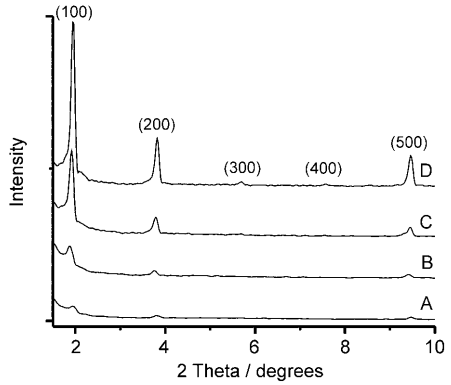

Figure 2. XRD patterns of mesoporous silica samples synthesized under different conditions: 1 TEOS/*n* $PyC_{12}Lys$/0.48 NaOH/112 H_2O, $n = 0.05$ (A), 0.10 (B), 0.20 (C), 0.40 (D).

n $PyC_{12}Lys$/0.48 NaOH/112 H_2O ($n = 0.05$, 0.10, 0.20, or 0.40). A set of evenly spaced reflections including one very intense peak at a small angle and four higher-order diffractions up to fifth order were detected. These peaks could be indexed as (100), (200), (300), (400), and (500) and are typical of the reflections of highly ordered lamellar structures.[12–14] XRD data reveal that a well-defined lamellar structure was achieved even at a very low concentration of $PyC_{12}Lys$, thus indicating that the lamellar mesostructure is highly accessible over a variety of preparation conditions using this new surfactant. The *d* spacing calculated from the position of the intense peak (100) gives a distance between the pore centers of approximately 4.55 nm, which is roughly twice the length of the surfactant in extended conformation. This result suggests that the surfactant chains are extended and well-ordered in two-dimensional space between the silica layers.

Complementary to the XRD data, transmission electron microscopy (TEM) further confirmed the formation of the lamellar mesostructure, as demonstrated by the interlaced aggregation of silica slits (Figure 3 A). More distinguishable is the scanning electron microscopy (SEM) image of the as-synthesized silica material, which displays large (tens of micrometers) shells with flat surfaces and clear faultages at the particle edges (Figure 3 B), unambiguously suggesting the lamellar structure.

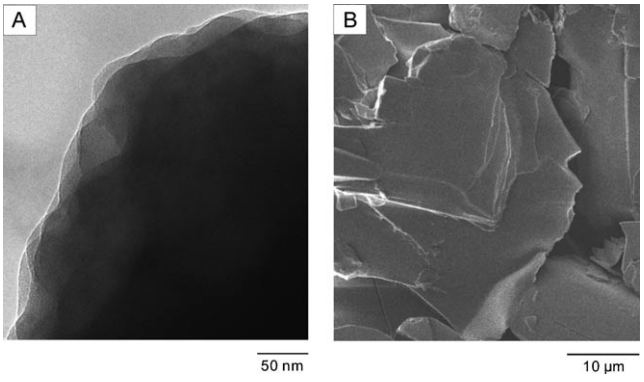

Figure 3. A) TEM and B) SEM images of as-synthesized lamellar mesostructured silica.

The conversion of the pyrrole moieties preorganized within the 2D space of the lamellar silica framework into ultrathin conjugated polypyrrole films was accomplished using $FeCl_3$ and subsequently ammonium persulfate. In this case, $FeCl_3$ acted as both oxidant for pyrrole polymerization and catalyst for further carbonization, while ammonium persulfate was used as oxidant to further facilitate the cross-linking of the formed polypyrrole chains, which was expected to yield 2D polypyrrole films with larger area. After 30 min reaction, a brown solid was collected by filtration and dried in air. As confirmed by XRD, TEM, and SEM (Figure S1 A–C in the Supporting Information), the mesostructure of the treated silica was maintained. An FTIR study revealed that α–α coupling of the pyrrole units occurred, and conjugated polypyrrole (PPy) was formed in the confined space (Figure S2 in the Supporting Information). UV/Vis spectroscopy further confirmed the formation of conjugated PPy. The as-synthesized silica does not exhibit any absorption in the range from 350 to 700 nm. After polymerization, the characteristic π–π* absorption of conjugated PPy at 390 nm was detected (Figure S3 in the Supporting Information).[15–17] Direct visualization of the encapsulated PPy films was realized after the removal of the silica framework using HF. TEM reveals a large amount of ultrathin films (Figure S1 D in the Supporting Information). The size of these films is comparable to the particle size of the silica host, suggesting that the channels and the formed PPy run the entire length of the particles. Owing to the spatial confinement of the silica framework, the PPy films in channels were stretched and isolated from each other, providing a prerequisite for producing pure single-layer graphene nanosheets after carbonization. Advantageously, after the polymerization process a considerable amount of complexed iron remained in the silica sample, as indicated by energy-dispersive X-ray spectroscopy. This iron could be conveniently used to enhance the formation of graphene during the carbonization process. Therefore, in our case, it is found that the confined PPy films, in the presence of iron complexes, can form a graphene structure at a low temperature (ca. 800 °C) in N_2 atmosphere.

Figure 4 A–C shows the TEM images of the resultant carbon films after the removal of the silica framework using diluted HF solution (2 %). As expected, many graphene sheets with lateral dimensions of hundreds of nanometers were observed on the top of the copper grid (Figure 4 A). Large sheets resemble crumpled silk veil waves, as reported.[18] They are transparent and are very stable under the electron beam (Figure 4 B). In the high-resolution TEM image, the surface of these nanosheets seems very smooth (Figure 4 C). Normal-incidence selected-area electron diffraction (SAED) was performed on this smooth region. The SAED pattern is shown in Figure 4 D. The well-defined six-fold-symmetry diffraction pattern is similar to that of peeled-off graphene[19] and confirms the crystalline structure of the obtained graphene nanosheets. On the other hand, the fact that the {1100} spots appear to be more intense than the {2110} spots further reflects the single-layer nature of the resulting graphene.[8] It should be noted that, owing to the intrinsic

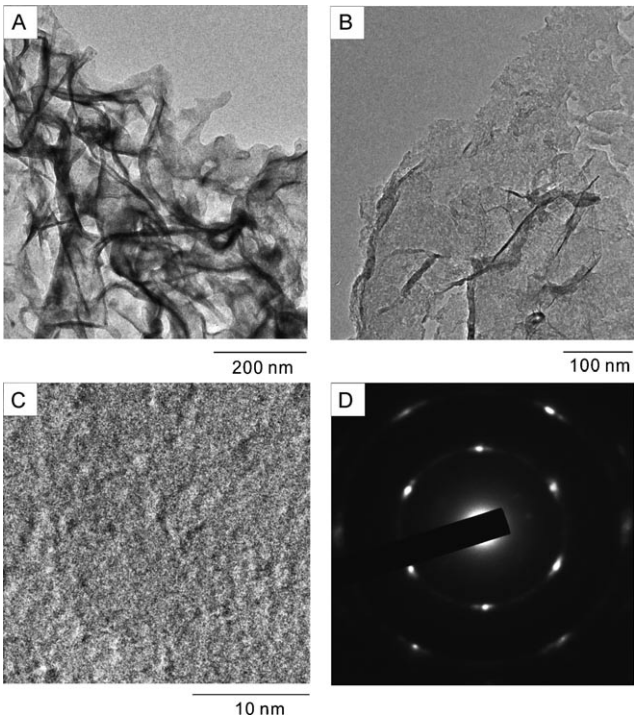

Figure 4. A–C) TEM images of large graphene sheets at different magnifications. D) Electron diffraction pattern of the graphene sheet in (B).

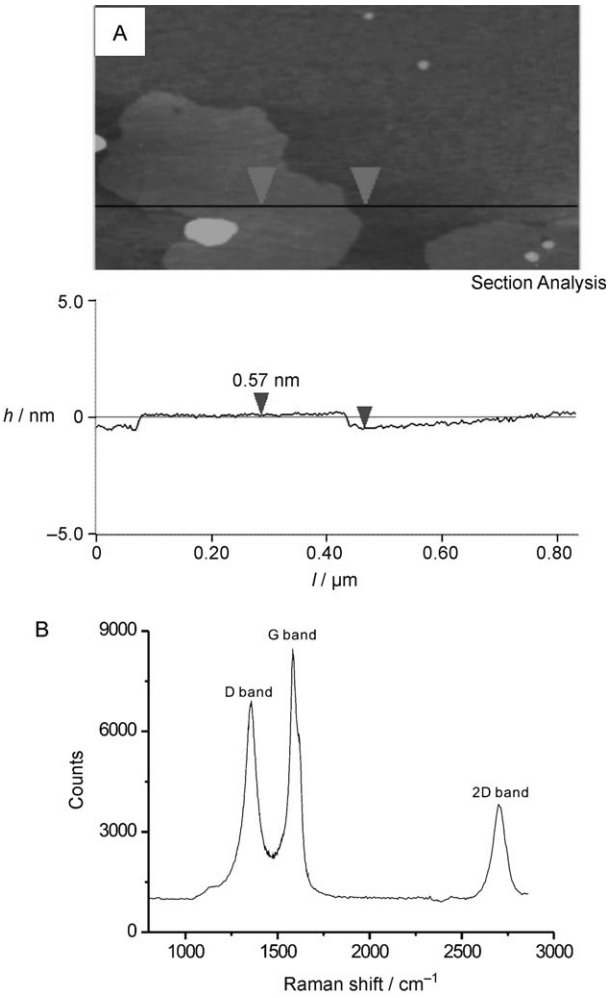

Figure 5. A) AFM image and corresponding height profile and B) Raman spectrum of the fabricated graphene nanosheet.

character of our method, pure single-layer graphene nanosheets (100%) were obtained, in contrast to reported chemical approaches, which produce large amounts of bilayer or multilayer graphene sheets along with single-layer graphene.[6–11]

The single-layer nature of the graphene is confirmed by atomic force microscopy (AFM, Figure 5A). The thickness of the graphene sheet is about 0.57 nm, comparable to that of the typical single-layer exfoliated sheets prepared by the annealing method in ultrahigh vacuum (0.6 nm).[20] The fact that the fabricated graphene is much thinner than most reported graphene sheets clearly implies that relatively clean graphene sheets were produced using our method. Nevertheless, the apparent 0.3 nm discrepancy in thickness compared to the theoretical value (0.34 nm) for graphene still suggests the presence of some residual foreign groups or structural defects on the sheets.

The Raman spectrum of the obtained graphene (Figure 5B) shows two peaks at 1350 and 1580 cm^{-1}. The peak at 1580 cm^{-1} (called the G band) corresponds to an E_{2g} mode of graphite and is related to the in-plane vibration of sp^2-bonded carbon atoms in a 2D hexagonal lattice, while the peak at 1350 cm^{-1} (called the D band) is associated with vibrations of carbon atoms with sp^3 electronic configuration of disordered graphite.[10] The intensity ratio of the D and G bands (I_D/I_G) of graphitic sheets is about 0.76, indicating a higher graphitization degree in the prepared samples. Remarkably, a relatively sharp and symmetric peak was detected in the Raman spectrum at 2698 cm^{-1} (called the 2D band), which is generated from a two-phonon double-resonance Raman process. In agreement with the observation in TEM and AFM, the occurrence and the shape of the 2D band further verified the single-layer structure of the fabricated graphene,[8,21] confirming the quality of our samples.

Interestingly, without any other treatment, after the removal of the silica framework the single-layer graphene sample could be easily dispersed in ethanol upon sonication. The dispersion is very stable and persisted for several days with no obvious precipitation (Figure 6A). This property made it easy to process the sample for practical applications. The UV/Vis absorption spectrum of the solution was also recorded (Figure 6B). The spectrum shows two peaks: besides a broad peak at 273 nm characteristic of π–π^* electron transition in the polyaromatic system of graphene layers, a sharp peak at 222 nm was also found, which is probably related to π–π^* electron transition in the polyene-type structure from the defects of the graphene sheets.[22]

The composition of the prepared graphene was studied by X-ray photoelectron spectroscopy (XPS). In the spectrum (Figure 7A), only signals denoting the presence of carbon and oxygen were detected. The atomic percentages are C1s 94.93% and O1s 5.07%, thus confirming the high carbon content. The C1s spectrum of the sample could be deconvo-

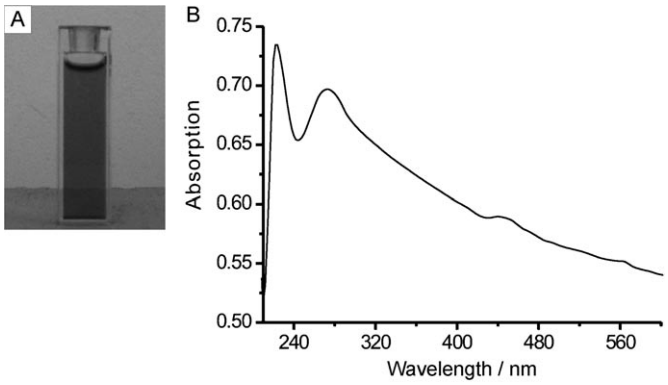

Figure 6. A) Photograph and B) UV/Vis spectrum of the obtained graphene nanosheets dispersed in ethanol.

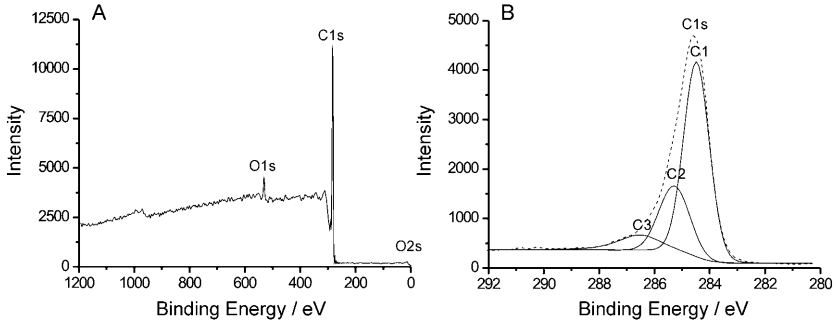

Figure 7. A) Survey X-ray photoelectron spectrum and B) C1s spectrum of obtained graphene nanosheets.

luted into three peaks (Figure 7B). The main peak located at a binding energy of 284.4 eV is related to the C–C bonding (sp^2 carbon, C1) in defect-free graphite. It is much larger than the peak associated with defect carbon (C2) at 285.3 eV and the peak at 286.5 eV related to carbon in C–O bonding (C3), thus indicating the presence, but small amount, of defects in our sample.[23] Table S1 in the Supporting Information displays the peak assignment and the corresponding relative areas from the curve fitting of the C1s spectrum.

The preliminary results described above are encouraging. Furthermore, previous research shows that the I_G/I_D ratio increased significantly with increasing pyrolysis temperature.[24] Therefore, after the optimization of the preparation conditions, the resulting graphene should have a more perfect structure.

In summary, we have developed an efficient strategy for producing pure single-layer graphene nanosheets based on a confined self-assembly approach. The crucial point of this strategy is the utilization of a confined space for individually producing single-layer graphene sheets. Besides the capability to fabricate clean and pure single-layer graphene that has been inaccessible by reported methods, the bottom-up approach described herein has many advantages, such as the use of mild preparation conditions and the avoidance of hazardous materials. Moreover, the preparation procedure is controllable and can be used to produce graphene on a gram scale. We believe that our findings represent an important development in the preparation of high-quality graphene on a large scale, which may significantly facilitate the application of graphene in a wide range of areas. Systematic investigation is ongoing.

Experimental Section

Preparation of mesostructured silica with $PyC_{12}Lys$ as the structure-directing agent: Lamellar mesostructured silica was prepared in basic medium through hydrothermal synthesis using TEOS as the silica source and $PyC_{12}Lys$ as the structure-directing agent and monomer. In a typical synthesis, $PyC_{12}Lys$ (1.95 g) was dissolved in deionized water (24 mL) with sodium hydroxide (0.22 g). The solution was stirred slowly for 1.5 h. Then TEOS (2.5 g) was added dropwise at room temperature. The molar compositions of the starting mixtures were 1 TEOS/0.40 $PyC_{12}Lys$/0.48 NaOH/112 H_2O. The resulting mixture was stirred at room temperature for 2 h and then transferred into an autoclave and heated at 85 °C for three days. After hydrothermal treatment, the mixture was filtered, and the resulting white powder was washed with Millipore water and acetone. The sample was dried in air at room temperature. The yield was about 2.5 g.

Preparation of PPy thin films within mesostructured silica frameworks: As-synthesized lamellar mesoporous silica (1.0 g) was dispersed in chloroform (25 mL) with vigorous stirring at room temperature, and then chloroform (10 mL) containing $FeCl_3$ (1.0 g) and ethanol (0.50 mL) was added to convert the densely packed pyrrole moieties within the silica into conjugated PPy nanosheets. After stirring for 1 h, ammonium persulfate (0.5 g) was added to the mixture to further polymerize the pyrrole moieties. The formed black solid was collected by filtration, washed thoroughly with water, and dried in air. The yield was about 1.2 g.

Preparation of single-layer graphene within confined silica pores: To obtain graphene, silica with the formed PPy nanosheets (1.0 g) was pyrolyzed in a nitrogen flow at 800 °C for 6 h. The silica frameworks were removed using aqueous HF (2%), and then the residue was collected, rinsed thoroughly with Millipore water and acetone, and dried in the air for further experiments. The yield of the resulting graphene material was 0.11 g.

Received: May 4, 2009
Published online: July 2, 2009

Keywords: graphene · mesostructured silica · polymerizable surfactants · self-assembly · template synthesis

[1] A. K. Geim, K. S. Novoselov, *Nat. Mater.* **2007**, *6*, 183.
[2] J. S. Bunch, A. M. van der Zander, S. S. Verbridge, I. W. Frank, D. M. Tanenbaum, J. M. Parpia, H. G. Craighead, P. L. McEuen, *Science* **2007**, *315*, 490.
[3] F. Schedin, A. K. Geim, S. V. Morozov, E. W. Hill, P. Blake, M. I. Katsnelson, K. S. Novoselov, *Nat. Mater.* **2007**, *6*, 652.
[4] X. Du, I. Skachko, A. Barker, E. Y. Andrei, *Nat. Nanotechnol.* **2008**, *3*, 491.
[5] K. S. Novoselov, A. K. Geim, S. V. Morozov, D. Jiang, Y. Zhang, S. V. Dubonos, I. V. Grigorieva, *Science* **2004**, *306*, 666.
[6] D. Li, M. B. Muller, S. Gilje, R. B. Kaner, G. G. Wallace, *Nat. Nanotechnol.* **2008**, *3*, 101.
[7] X. Fan, W. Peng, Y. Li, X. Li, S. Wang, G. Zhang, F. Zhang, *Adv. Mater.* **2008**, *20*, 1.

[8] Y. Hernandez, V. Nicolosi, M. Lotya, F. M. Blighe, Z. Sun, I. T. McGovern, B. Holland, M. Byrne, Y. K. Gun′ko, J. J. Boland, P. Niraj, G. Duseberg, S. Krishnamurthy, R. Goodhue, J. Hutchison, V. Scardaci, A. C. Ferrari, J. N. Coleman, *Nat. Nanotechnol.* **2008**, *3*, 563.
[9] Y. Si, E. T. Samulski, *Nano Lett.* **2008**, *8*, 1679.
[10] G. Wang, J. Yang, J. Park, X. Gou, B. Wang, H. Liu, J. Yao, *J. Phys. Chem. C* **2008**, *112*, 8192.
[11] J. T. Robinson, F. K. Perkins, E. S. Snow, Z. Wei, P. E. Sheehan, *Nano Lett.* **2008**, *8*, 3137.
[12] M. Antonietti, D. Kuang, B. Smarsly, Y. Zhou, *Angew. Chem.* **2004**, *116*, 5096; *Angew. Chem. Int. Ed.* **2004**, *43*, 4988.
[13] A. Shimojima, Z. Liu, T. Ohsuna, O. Terasaki, K. Kuroda, *J. Am. Chem. Soc.* **2005**, *127*, 14108.
[14] A. M. Seddon, H. M. Patel, S. L. Burkett, S. Mann, *Angew. Chem.* **2002**, *114*, 3114; *Angew. Chem. Int. Ed.* **2002**, *41*, 2988.
[15] H. Uehara, M. Miyake, M. Matuda, M. Sato, *J. Mater. Chem.* **1998**, *8*, 2133.
[16] N. Yanai, T. Uemura, M. Ohba, Y. Kadowaki, M. Maesato, M. Takenaka, S. Nishitsuji, H. Hasegawa, S. Kitagawa, *Angew. Chem.* **2008**, *120*, 10031; *Angew. Chem. Int. Ed.* **2008**, *47*, 9883.
[17] T. Bein, P. Enzel, *Angew. Chem.* **1989**, *101*, 1737; *Angew. Chem. Int. Ed. Engl.* **1989**, *28*, 1692.
[18] M. D. Stoller, S. Park, Y. Zhu, J. An, R. S. Ruoff, *Nano Lett.* **2008**, *8*, 3498.
[19] J. C. Meyer, A. K. Geim, M. I. Katsnelson, K. S. Novoselov, T. J. Booth, S. Roth, *Nature* **2007**, *446*, 60.
[20] D. Graf, F. Molitor, K. Ensslin, C. Stampfer, A. Jungen, C. Hierold, L. Wirtz, *Nano Lett.* **2007**, *7*, 238.
[21] Z. Ni, Y. Wang, T. Yu, Z. Shen, *Nano Res.* **2008**, *1*, 273.
[22] Y. Liu, R. L. Vander Wal, V. N. Khabashesku, *Chem. Mater.* **2007**, *19*, 778.
[23] J. I. Paredes, A. M. Alonso, J. M. Tascon, *Langmuir* **2007**, *23*, 8932.
[24] J. Jang, H. Yoon, *Adv. Mater.* **2003**, *15*, 2088.

